

D. Mazon, J. Blum, C. Boulbe, B. Faugeras, M. Baruzzo, A. Boboc, S. Bremond,
M. Brix, P. DeVries, S. Sharapov, L. Zabeo and JET EFDA contributors

EQUINOX: A Real-Time Equilibrium Code and its Validation at JET

“This document is intended for publication in the open literature. It is made available on the understanding that it may not be further circulated and extracts or references may not be published prior to publication of the original when applicable, or without the consent of the Publications Officer, EFDA, Culham Science Centre, Abingdon, Oxon, OX14 3DB, UK.”

“Enquiries about Copyright and reproduction should be addressed to the Publications Officer, EFDA, Culham Science Centre, Abingdon, Oxon, OX14 3DB, UK.”

The contents of this preprint and all other JET EFDA Preprints and Conference Papers are available to view online free at www.iop.org/Jet. This site has full search facilities and e-mail alert options. The diagrams contained within the PDFs on this site are hyperlinked from the year 1996 onwards.

EQUINOX: A Real-Time Equilibrium Code and its Validation at JET

D. Mazon¹, J. Blum², C. Boulbe², B. Faugeras², M. Baruzzo³, A. Boboc⁴,
S. Bremond¹, M. Brix⁴, P. DeVries⁴, S. Sharapov⁴, L. Zabeo⁴
and JET EFDA contributors*

JET-EFDA, Culham Science Centre, OX14 3DB, Abingdon, UK

¹ Association EURATOM-CEA, CEA Cadarache, DSM/IRFM 13108 St Paul Lez Durance Cedex France

² Laboratoire J-A Dieudonné (UMR 66 21), Université de Nice Sophia-Antipolis,
CNRS Parc Valrose 06108 Nice Cedex 02 France

³ Association EURATOM/UKAEA, Culham science centre Abingdon Oxon OX14 3DB UK

⁴ Consorzio RFX-Associazione EURATOM ENEA per la Fusione, I-35127 Padova, Italy.

* See annex of F. Romanelli et al, "Overview of JET Results",
(Proc. 22nd IAEA Fusion Energy Conference, Geneva, Switzerland (2008)).

Preprint of Paper to be submitted for publication in Proceedings of the
4th International Scientific Conference on Physics and Control
(1st September 2009 - 4th September 2009)

1. INTRODUCTION

The real-time reconstruction of the plasma magnetic equilibrium in a Tokamak is a key point to access high performance regimes. Indeed, the shape of the plasma current density profile is a direct output of the reconstruction and has a leading effect for reaching a steady-state high performance regime of operation. The challenge is thus to develop methods and algorithms that reconstruct the magnetic equilibrium in the perspective to use these outputs for feedback control purposes.

But in present days tokamaks only the shape of the plasma boundary is routinely identifiable in real-time in less than few milliseconds using a set of magnetic and diamagnetic coils spread around the vessel. This information is mainly used for controlling the plasma shape in realtime during a plasma discharge using coils current in a feedback control loop. The idea is to achieve a required shape and to maintain it in a stationary manner in order to avoid for example sudden termination of the plasma when the plasma touches the first wall. In JET the so-called XLOC code is used routinely for plasma shape control [1]. Based on this JET flux boundary code confinement parameters are deducted like the diamagnetic energy, the internal inductance and plasma separatrix geometry in less than 1ms. But with this algorithm it is not possible to compute the internal magnetic flux configuration which is needed if we want to analyze the phenomenon occurring in the interior of the plasma. In this case the only way to get access to the current density profile is to use off-line codes that can compute accurately the profile but with no possibility to act in real time on it. This is rather a strong limitation because we know from the analysis performed that the shape of the current density profile is one of the key element to enhance the plasma performance. We have seen in particular that non monotonic current density profiles can trigger enhanced particles and heat confinement [2]. On top of this the current density profile has a resistive diffusion time and any variation of the current drive systems takes some time to be efficient. So it is clear that by controlling in real time such a profile, taking into account the effect of disturbances that tends to adversely affect the time behaviour of the controlled variables, we insure stability but also performance [3, 4].

2. MATHEMATICAL FORMULATION OF THE PLASMA EQUILIBRIUM

The problem of plasma equilibrium in a Tokamak is a free boundary problem in which the plasma boundary is defined as the last closed magnetic flux surface. Inside the plasma, the equilibrium equation in an axisymmetric configuration is called the Grad-Shafranov equation [5, 6]. This equation is derived from the combination of the magnetostatic Maxwell's equations which are satisfied in the whole of space in presence of a magnetic field and the equilibrium of the plasma itself which occurs when the kinetic pressure is equal to the Lorentz force of the magnetic pressure. The expression of the Grad-Shafranov equation in a cylindrical coordinates system (r, z, ϕ) where $r=0$ is the major axis of the torus reads:

$$-\Delta^* \psi = rp'(\psi) + \frac{1}{\mu_0 r} (ff')(\psi) \quad \text{with} \quad * = \frac{\partial}{\partial r} \left(\frac{1}{\mu_0 r} \frac{\partial}{\partial r} \right) + \frac{\partial}{\partial z} \left(\frac{1}{\mu_0 r} \frac{\partial}{\partial z} \right) \quad (1)$$

Where μ_0 is the magnetic permeability of the vacuum, $\psi(r,z)$ the poloidal flux and f the diamagnetic function. The right hand side of equation (1) is a non-linear source which represents the toroidal component of the plasma current density. It involves the functions $p(\psi)$ and $f(\psi)$ which are not directly measured inside the plasma. Assuming that Dirichlet boundary conditions, h , are given on Γ which is the poloidal cross section of the vacuum vessel, the final equations governing the behavior of $\psi(r,z)$ inside the vacuum vessel become:

$$-\Delta^* \psi = \left[\frac{r}{R_0} A(\bar{\psi}) + \frac{R_0}{r} B(\bar{\psi}) \right] \text{ defining } A(\bar{\psi}) = p'(\bar{\psi}) \text{ and } B(\bar{\psi}) = \frac{1}{\mu_0 r} (ff')(\bar{\psi}) \quad \psi = h \text{ on } \Gamma \quad (2)$$

The entire problem is thus resumed to identify in real time the plasma current i.e. the non linear functions A and B (function of the normalized flux in the previous equation)

3. THE EQUINOX CODE

In order to meet the real-time requirements, a new version of the code called Equinox has been design and implemented in C++ using a finite element method and a non linear fixed point algorithm associated to a least square optimization procedure. The code relies on tokamak specific software like XLOC providing flux values on the first wall of the vacuum vessel. By means of least-square minimization of the difference between measurements and the simulated ones the code identifies the source term of the non linear Grad-Shafranov equation. The experimental measurements that enable the identification are the magnetics on the vacuum vessel, the interferometric and polarimetric measurements on several chords and the motional Stark effect measurements. For the magnetic measurements the flux loops give the poloidal flux on particular nodes M_i such that $\psi(M_i) = h_i$ on Γ . Thanks to an interpolation (performed by XLOC at JET) between the points M_i these measurements provide the Dirichlet boundary condition h . The problem is thus resumed to find a solution that minimizes the cost function defined as:

$$J(A, B, n_e) = J_1 + K_1 J_1 + K_2 J_2 + J_{\mathcal{E}}$$

With

$$J_0 = \sum_i \left(\frac{1}{r} \frac{\partial \psi}{\partial n}(N_i) - g_i \right)^2; \quad J_1 = \sum_i \left(\int_{C_i} \frac{n_e}{r} dl - \alpha_i \right)^2; \quad J_2 = \sum_i \left(\int_{C_i} n_e dl - \beta_i \right)^2$$

Where g_i , α_i and β_i are respectively the measurements of the magnetic poloidal field, the Faraday rotation and the line integrated density along the chords C_i . The weighting parameters K_1 to K_2 enable to give more or less importance to the corresponding experimental measurements [8]. As the inverse problem of the determination of A and B is an ill posed one a Tikhonov regularization term [9] $J_{\mathcal{E}}$ constrains the functions A , B and n_e (n_e being the plasma density) to be smooth enough and its expression is given by the following expression:

$$J_{\varepsilon} = \varepsilon_1 \int_0^1 [A''(x)]^2 dx + \varepsilon_2 \int_0^1 [B''(x)]^2 dx + \varepsilon_3 \int_0^1 [n_e''(x)]^2 dx$$

where ε_1 , ε_2 and ε_3 are the regularizing parameters. Equation (2) is solved using a finite element method [10]. The finite element solver uses P1 triangles, the calculation being limited to the vacuum chamber. A careful implementation leads to execution time less than 60ms per iteration on a 2GHz PC, complemented with excellent robustness. The unknown functions A , B , n_e are approximated by decomposition in a reduced basis. The basis can be made of different types of functions (polynomials, B-splines, wavelets etc) [11]. In our case we choose B-splines. Let u be the vector which contains the coordinates of A , B and n_e in the chosen basis. The Picard type (fixed point) algorithm is then used to solve iteratively the inverse and direct problem. The discretisation of the equation (2) can be written as:

$$K\psi = D(\psi)u + h \quad (3)$$

Where D is the plasma current matrix, K is the stiffness matrix and h is due to the Dirichlet boundary conditions. The discrete inverse optimization problem is to find u minimizing the cost function which can be written as

$$J(u) = \|C(\psi)\psi - k\|^2 + u^T \Lambda u$$

while ψ satisfies (3). The quantity $C(\psi)\psi$ represents the outputs of the model, k the experimental measurements, $C(\psi)$ is the observation operator. The matrix Λ represents the regularization terms. In order to solve this problem we use an iterative algorithm based on fixed point iteration. At the n^{th} iteration ψ_n and u_n are given. The non linear mapping between $\psi(u)$ and u is given by the relation:

$$\psi = K^{-1} [D(\psi_n)u + h]$$

and the cost function to be minimized is given by

$$J(u) = \|C(\psi)\psi - k\|^2 + \|u^T \Lambda u\|$$

This last equation is used to determine ψ_{n+1} . Then fixed point iteration for equation (3) enables to find ψ_{n+1} .

$$\psi_{n+1} = K^{-1} [D(\psi_n)u_{n+1} + h]$$

Since the algorithm is initialized from the equilibrium at the previous time step two or three point iterations are usually enough to ensure convergence. This leads to a very efficient algorithm.

4. EQUINOX VALIDATION

The validation of the Equinox code has been performed starting from a database of about 130

pulses, well representative of the JET discharges with different shape and triangularity of the plasma boundary and with global parameter varying in the whole JET interval. For some pulses clear MHD signatures have been identified and help in particular at the validation of the current density profile. The strategy of the validation has been applied to the two versions of the codes. The first one called Equinox-M is the version using only the inputs from the magnetic measurement via XLOC. This version gives accurate plasma geometry and global parameters and does not intend to give very precise information about the current density profile. The second version Equinox-J includes internal measurements like polarimetry or MSE and is able to identify hollow plasma current density profiles. The validation of the Equinox-M version has been done mainly using the results of the well assessed EFIT equilibrium code [12] constraint by magnetic measurements only which is used in a routinely manner at JET for intershot analysis. The shape of the plasma is fairly well reproduced as it can be seen in Fig. 1 and 2 for the upper triangularity and plasma volume. For the spatial location of the plasma several checks have been made like the comparison of the coordinates R_x and Z_x of the X point, the different gaps at some poloidal locations (defined as the distance between the plasma boundary and the vessel) see Fig. 3 and 4. The error remains very low for the X point position but important differences can be seen for the right outer gap.

In order to validate this result we decided to compare the ROG obtained by equinox with the XLOC one. Indeed as our code is a free boundary code which means that no assumption is made on the plasma shape we are able to compare the shape parameters of our reconstruction with the one obtained by XLOC itself. Results of that comparison can be seen in Fig.5. Agreement is found with XLOC which tends to demonstrate that EFIT is less precise for the ROG reconstruction. At that stage it was necessary to investigate global quantities characteristic of the current density profile.

Global quantities like the internal inductance l_i are compared in Fig.6. Some differences can be noted for the internal inductance the medium error value being around 0.1. In order to quantify the sensibility of the Equinox output to the error on the measurements we perturbed by 1% the inputs data from XLOC and get a standard deviation of about 0.1 for the l_i as seen in Fig.7. So the difference observed on l_i between EFIT and Equinox is of the order of the error bars on the results. In terms of q profile this difference is small on the particular case of Pulse No: 74937 in Fig.8. We can note in particular that the main difference comes from the q_{ax} which is one of the consequences of the lack of information coming from the internal part of the plasma.

Finally in order to fully assess the Equinox-M reconstruction we have used PROTEUS [7] that solves the direct problem of the Grad Shafranov equation. The idea is to compute the flux mapping starting from a given and known current density profile. In that particular case a monotonic current density profile was chosen, the equilibrium has been reconstructed by PROTEUS who computed also the boundary conditions requested by Equinox. The outputs of Equinox are then compared with the ones coming from PROTEUS. A very good agreement is found as it can be seen in the following table in particular for the plasma volume, l_i and q profile confirming that the statistic relies on a very strong and accurate computation.

	PROTEUS	EQUINOX
I_p	2e6	2e6
r_{mag}	3.0620	3.0691
z_{mag}	0.2972	0.2983
psia	-0.2896	-0.3468
rx	2.5310	2.5279
zx	-1.4180	-1.4248
psib	-1.0588	-1.0605
β_p	1.9050	1.7846

	PROTEUS	EQUINOX
L_i	0.7470	0.7095
Q_0	1.1550	1.8256
Q_{95}	5.4710	5.3508
Trianu	0.4290	0.4075
Trianl	0.3720	0.3861
Vol	74.7080	74.3860
Surf	4.2520	4.2329
Perimeter	8.2750	7.9232
rgeom	2.8725	2.8726

In the case of the Equinox-J version the same results were obtained for the validation of the plasma shape and position, which were not modified by the inclusion of internal measurements. More interesting was to validate the obtained current density profile. The first strategy was to use clear MHD signatures of some shots of the database for checking the location of the corresponding mode. An example can be seen in Fig.9 where the location of the $q=1.5$ mode is given in blue by Equinox and in green identified from Fourier analysis of the magnetic measurements and electron temperature (Electron Cyclotron Emission). The agreement is almost perfect. The second strategy, see Fig.8 for example, was for the other shots of the database to compare the Equinox (red line) reconstruction with some reconstruction using EFIT constraint by MSE (green line). In dotted lines are represented for the same shot at the same time the profiles obtained with magnetic only. Here again the agreement is very good.

CONCLUSION

A new real-time solver of the Grad-Shafranov equation called Equinox has been developed and validated at JET. It integrates internal measurements like polarimetry and MSE to reconstruct the plasma equilibrium in less than 50ms. This code is written in C⁺⁺ and is now about to be implemented into the JET Real-time system. This opens brand new set of very interesting experiments about discharge performance optimisation.

REFERENCES

- [1]. D.P O'Brien, "Local expansion method for fast plasma boundary identification in JET", Nuclear Fusion, Vol **33** (3) p331 (1993)
- [2]. X. Litaudon, "Progress towards steady-state operation and real-time control of internal transport barriers in JET", Nuclear Fusion, Vol.**43**, No.7, July 2003, p.565-572

- [3]. D..Mazon,“Active control of the current density profile in JET” Plasma Physics and Controlled Fusion, Vol.**45**, No.7, July 2003, p.L47-L54.
- [4]. D. Moreau,” A two-time-scale dynamic-model approach for magnetic and kinetic profile control in advanced tokamak scenarios on JET” Nuclear Fusion, Vol.**48**, No.10, October 2008, p.106001
- [5]. H.Grad, “Hydromagnetic equilibria and force free fields”, 2nd U.N conference on the peaceful uses of Atomic energy, Geneva 1958 Vol **31** pp 190-197.
- [6]. V. Shafranov, Soviet Physics JETP **6** 1013 (1958)
- [7]. H.Grad Physical Review Letter **24** pp 1337-1340 (1970)
- [8]. J. Blum, Nuclear Fusion **30** 1475 (1990)
- [9]. A. Tikhonov, “Solutions of ill-posed problems” Winston, Washington D.D (1977)
- [10]. P. Ciarlet, “The finite element method for elliptic problems”, North Holland, (1980)
- [11]. J. Blum, “An inverse problem in plasma physics: the identification of the current density profile in a tokamak”, in IMA Volumes in Mathematics and its applications, Large scale optimization with applications, Part 1: optimization in inverse problems and design, edited by Biegler, Coleman, Conn and Santosa, 1997, Vol 92 pp 17-36
- [12]. L. Lao, Nuclear Fusion **30** 1035 (1990)
- [13]. Albanese R., “*Numerical Studies of the Next European Torus via the PROTEUS Code.* - 12th Conference on the Numerical Simulation of Plasmas, S. Francisco, Sept. 1987.

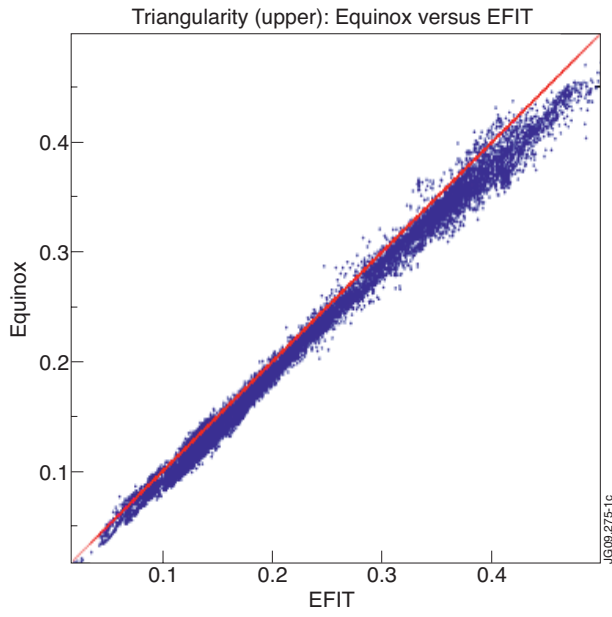


Figure 1: Comparison EFIT versus Equinox for the upper triangularity.

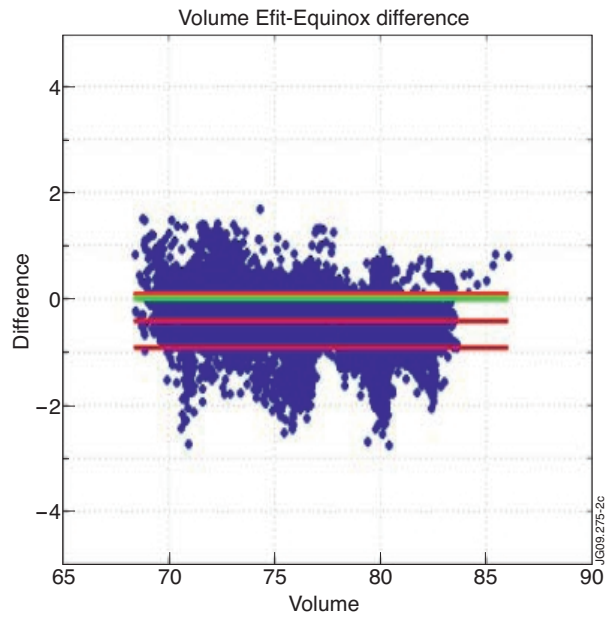


Figure 2: Standard deviation between EFIT and Equinox for the plasma volume (m^3)

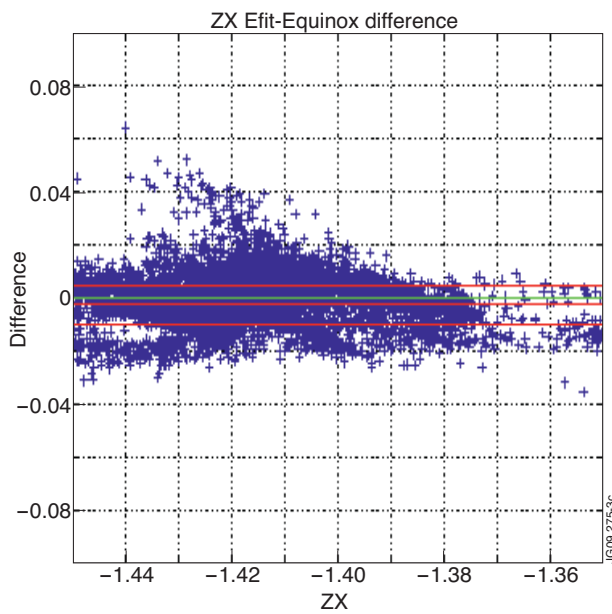


Figure 3: Comparison between EFIT and Equinox for the Z position of the X point.

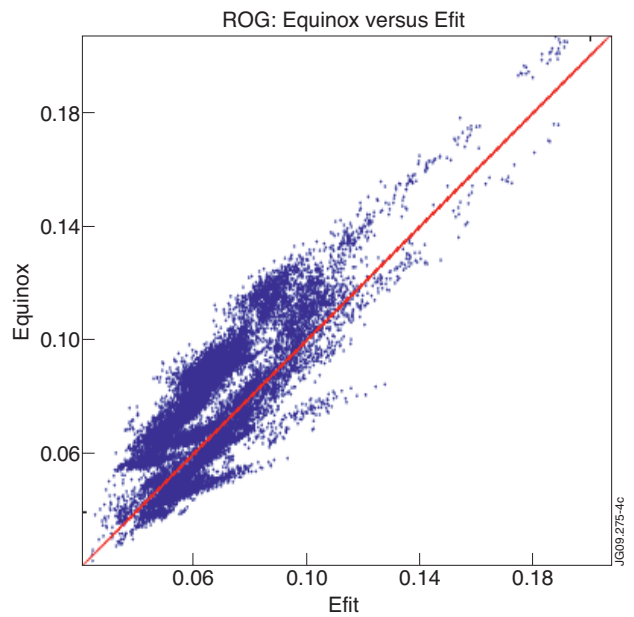


Figure 4: Comparison between EFIT and Equinox for the ROG (Right Outer Gap) in meter.

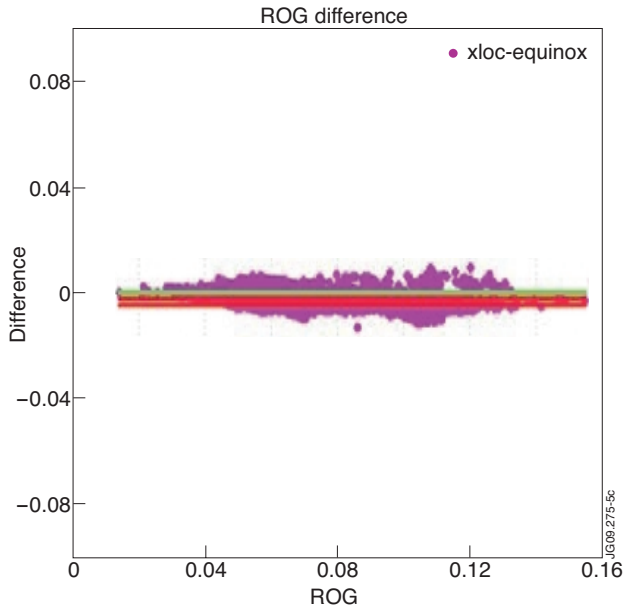


Figure 5: Comparison between XLOC and Equinox for the ROG.

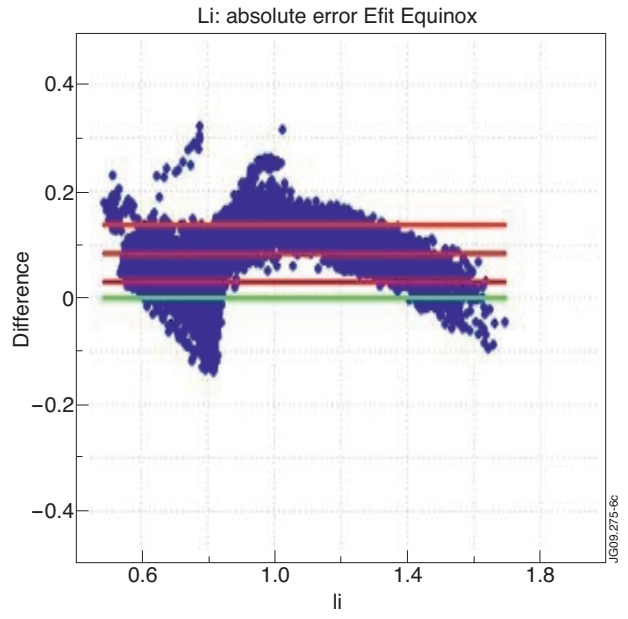


Figure 6: Comparison between EFIT and Equinox for the internal inductance l_i .

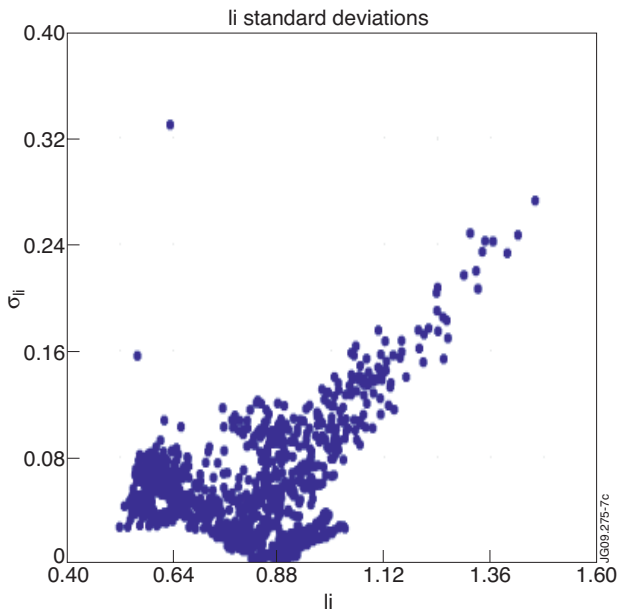


Figure 7: Standard deviation of l_i with random variation of the original inputs.

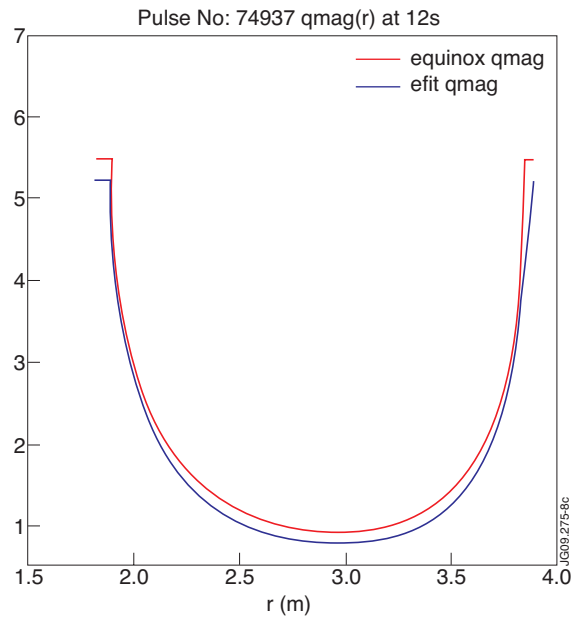


Figure 8: Comparison between EFIT and Equinox of the safety factor profile.

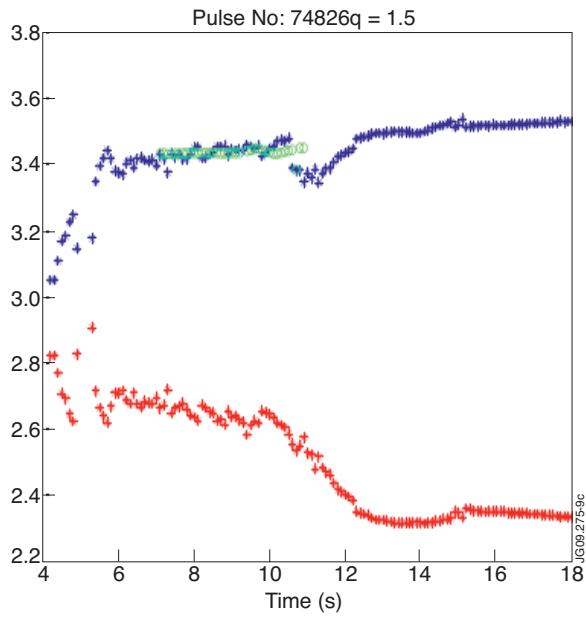


Figure 9: Time traces of the location of the $q=1.5$ surface as found by Equinox (red low field side and blue high field side) and in green location of that mode deduced from Fourier analysis of Magnetic and ECE data

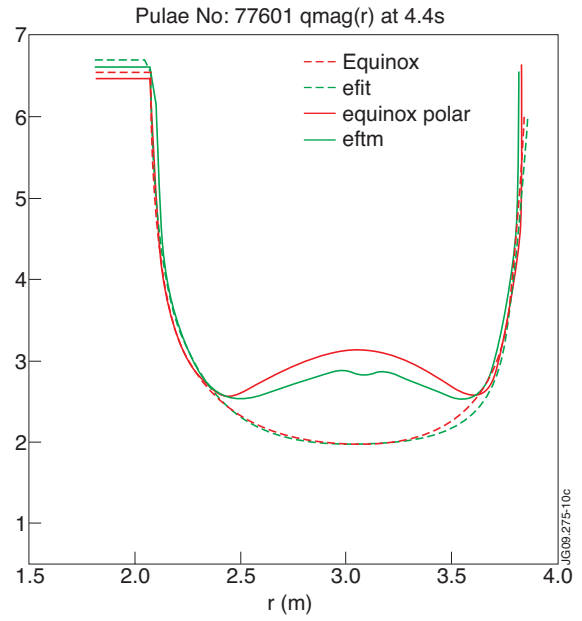


Figure 10: Profiles comparison between EFIT constraint by magnetic measurements (dotted green), by MSE (green line) and Equinox constraint by magnetic measurements (dotted red), by MSE (red line) for Pulse No: 77601 at $t = 4.4s$.